SCIENCE CHINA
Chemistry

• ARTICLES •

December 2013 Vol.56 No.12: 1701–1709
doi: 10.1007/s11426-013-4887-8

# Preparation of enzymatically cross-linked sulfated chitosan hydrogel and its potential application in thick tissue engineering

CHEN ZhiPing, WANG Wei*, GUO Lei, YU YanYan & YUAN Zhi*

*Key Laboratory of Functional Polymer Materials, Ministry of Education; Institute of Polymer Chemistry, Nankai University, Tianjin 300071, China*

Received March 15, 2013; accepted April 26, 2013; published online May 21, 2013

For the requirement of preliminary vascularization, the scaffolds for thick tissue engineering should have not only good cell affinity, but also anticoagulant ability. In this paper, enzymatically cross-linked hydrogel scaffolds based on sulfated chitosan (SCTS) were prepared. Firstly, sulfated chitosan-hydroxyphenylpionic acid (SCTS-HPA) conjugate was synthesized, and the structure of SCTS-HPA was identified by FITR and $^1$H NMR. And then the enzymatically cross-linked hydrogels were prepared in presence of horseradish peroxidase (HRP) and hydrogen peroxide ($H_2O_2$). The gelation time, mechanical property, morphology and cytotoxicity to human umbilical vein endothelial cells (HUVECs) of the hydrogel were evaluated *in vitro*, the tissue compatibility of SCTS-HPA scaffold was studied *in vivo*. The results showed that the gelation time, mechanical property, morphology of the dehydrated hydrogel could be controlled by the the concentration of HRP and $H_2O_2$. The cytotoxicity test showed that the hydrogel extracts have no cytotoxicity to HUVECs. The *in vivo* assay indicated that SCTS-HPA scaffold have good tissue compatibility with no thrombus formation. All these results indicated that the SCTS-HPA scaffold could be used as a thick tissue engineering scaffold.

**sulfated chitosan, horseradish peroxidase, anticoagulant, tissue compatibility**

## 1 Introduction

Tissue engineering holds the promise to generate artificial tissues or organs for regenerative medicine applications. Despite tremendous progresses have been achieved in this field, there are still serious challenges in creating 3-dimension scaffolds, especially for thick tissue engineering application. Relative to the thin tissue engineering, a thick tissue engineering scaffold should contain a highly branched vascular network for supporting nutrients to the deep cells [1]. The contact of the scaffold with blood may introduce thrombus formation. Therefore, the key requirements for thick tissue engineering scaffolds include not only the maintenance of cell viability and function, but also good blood compatibility, and the latter is more important.

Among the materials used for biomedical applications, chitosan (CTS), as a relatively less toxic, biocompatible and degradable natural glycosaminoglycan, has been widely used in tissue engineering and drug delivery system [2]. However, the application of chitosan is limited due to its poor solubility. Furthermore, the cationic groups in this polysaccharide have the venture to promote platelet adhesion and activation, and then result in thrombus formation [3]. Therefore, many CTS derivatives have been developed to enhance the solubility and blood compatibility, such as carboxymethyl chitosan (CMCTS) [4], polyethylene glycol (PEG) chitosan (PEG-CTS) [5]，sulfated chitosan (SCTS) [6], and so on. Among all the derivatives, the SCTS attracts lots of attention due to its similar structure to extracellular matrix molecules (ECMs), excellent ability of anticoagulation and good affinity to cells. Prager *et al*. [7] reported that fibroblasts adhered to and grew better on the SCTS containing scaffold than on the CTS containing scaffold. And Huang *et al*. [8] proved that the SCTS containing surface

*Corresponding authors (email: duruo@nankai.edu.cn; zhiy@nankai.edu.cn)

could reduce platelet adhesion/activation, and promote endothelial cell attachment/growth *in vitro*. All these results indicate that the SCTS has two fundamental properties, good hemacompatibility and cell affinity, which are benefits to the application in blood vessel containing thick tissue engineering.

Hydrogel is an ideal scaffold for thick tissue engineering for its high water-content and good permeability environment. Among the methods of hydrogel formation, enzyme-triggered hydrogel formation attracts much attention due to its mild formation conditions. In this study, we used HRP/$H_2O_2$ as catalyst/cross-linking agent and prepared enzymatically cross-linked sulfated chitosan hydrogel. The gelation time, mechanical property, and morphology of the hydrogel were evaluated. And the cytotoxicity to HUVECs of the hydrogel extracts was studied by MTT assay. The tissue compatibility of the hydrogel scaffolds was also evaluated by implanted the scaffolds into the subcutaneous pockets of SD female mice.

## 2 Experimental

### 2.1 Chemicals and apparatus

Chitosan (CTS) ($M_w$ = 50 kDa, *DD* > 95%) and carboxymethyl chitosan (CMCTS) ($M_w$ = 50 kDa, *DS* > 80%) were purchased from Ao'xing Biotech Co. Ltd. (Zhejiang, China) and used without further purification. Hydroxyphenylpionic acid (HPA) was purchased from Aladdin Chemistry Co., Ltd. (Beijing, China). $H_2O_2$ was supplied by Beifang medical chemistry regent factory (Tianji, China). 1-Ethyl-3-(3-dimethylaminopropyl) carbodiimide hydrochloride (EDC·HCl) and *N*-hydroxy-succinimide (NHS) were obtained from GL Biochem., Ltd. (Shanghai, China). Horseradish peroxidase (HRP) was purchased from Boyao biotech Co., Ltd. (Shanghai, China). [3-(4,5-Dimethylthiazol-2-yl)-2,5-diphenyltetrazoliumbromide] (MTT) was purchased from Dingguo biotechnology Co., Ltd. (Tianjin, China). DMSO was supplied by Fuchen chemistry regent factory (Tianjin, China). For cell culture, endothelial cell medium (ECM) containing 1% endothelial cell growth supplement (ECGS) and 1% penicillin/ streptomyclin solution (P/S), fetal bovine serum were supplied by Yuhengfeng biotech CO., Ltd. (Beijing, China).

The following apparatus was used, gel permeation chromatography (GPC) (Viscotek, United States), inductively coupled plasma-atomic emission spectrometer (ICP) (Jarrell-Ash, United States), Tensor 27 Fourier transform infrared spectrometer (FTIR) (Spectrum Instruments Co., Ltd., Brook, Germany), UNITY Plus-400 MHz NMR spectrometer (Varian, United States), Shimadzu SS-550 scanning electron microscopy (SEM) (Shimadzu, Japan), AR2000ex rheometer (TA Instruments, United States), Olympus BX51 fluorescence microscope (Olympus, Japan).

### 2.2 Synthesis of SCTS and SCTS-HPA conjugate

SCTS was synthesis according to the literature as showed in Figure 1 [9]. Briefly, 90 mL mixture of 95% $H_2SO_4$ and $HSO_3Cl$ (1:2, *v*/*v*) was prepared in an ice bath, after cooling for 30 min, 2 g CTS was added to the mixture. The ice bath was then removed and the solution was stirred for another 2 h. The product was precipitated by pouring the reaction mixture into cold diethyl ether. The precipitate was collected, and dissolved in water, neutralized with 1 M NaOH. The resulting product was purified using a dialysis tube ($M_w$ = 1.2–1.4 kDa) against distilled water for 3 days and lyophilized.

SCTS-HPA conjugate was prepared in the DMF/$H_2O$, using carbodiimide activation chemistry [10]. Firstly, 0.64 g SCTS was dissolved in DMF/$H_2O$ (3:1, *v*/*v*), followed by adding 0.55 g HPA. To active the carboxyl of HPA, EDC and NHS were dissolved in 20 mL DMF and added to the solution of SCTS. After stirring at room temperature for 24 h, the product was precipitated in acetone and then dialyzed against distilled water for 3 days and lyophilized.

### 2.3 Characterization of SCTS and SCTS-HPA

The molecular weight of SCTS was determined by GPC. The degree of substitution (DS) of the $-SO_3-$ group was calculated from the sulfur content in SCTS which was determined by ICP. The structure of SCTS-HPA was confirmed by FTTR and $^1$H NMR and the degree of substitution (DS) of HPA was determined by using $^1$H NMR.

### 2.4 Hydrogel preparation and gelation time test

SCTS-HPA hydrogels were prepared in 1 mL vials at room

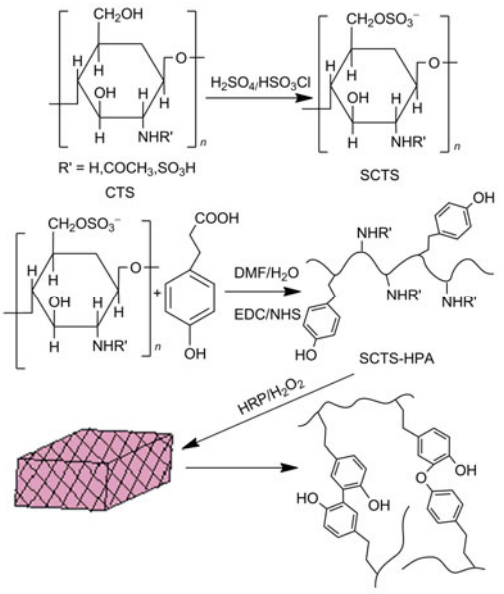


**Figure 1** Schematic illustration of SCTS-HPA preparation and hydrogel formation.

temperature. Briefly, 200 μL SCTS-HPA solution (4 wt%) was prepared in PBS (pH 7.4), and then 5 μL different concentration HRP and 5 μL different concentration of $H_2O_2$ were added, and the final concentration of SCTS-HPA and HRP was 3.8 wt%. The gelation time was determined using a vial tilting method. The gelation time was determined when the solution stop flowing for 1 min.

### 2.5 Rheological analysis

Dynamic rheological analysis of different cross-linking degree of hydrogels was performed on an AR2000ex rheometer. The measurements were taken at 37 °C in the dynamic mode with a constant strain of 1% and frequency of 1 rad/s. For the measurement, 400 μL SCTS-HPA solution (4 wt% in PBS) was placed on the plate of the rheometer, and 10 μL HRP and 10 μL different concentration of $H_2O_2$ were added. The solution was vortexed immediately, and started to test.

### 2.6 Morphology of dehydrated SCTS-HPA hydrogels

The microporous structure of the dehydrated hydrogels was determined by SEM. Hydrogels cross-linked with 1.5 units/mL HRP and different concentration of $H_2O_2$ were fabricated in a special mold. After fully cross-linked, the hydrogel specimens were freeze-dried under vacuum for 2 days at −50 °C. Then the samples were cross-sectioned using a sharp blade and sputter-coated with gold and finally imaged by using a Shimadzu SS-550 scanning electron microscope.

### 2.7 Cytotoxicity assay

The cytotoxicity of hydrogels was tested by incubating HUVECs with the 100% and 50% hydrogel extracts according to GB/T 16886.5-2003 (ISO10993-5:1999). Hydrogel extracts were prepared by adding hydrogel fragments to serum-free ECM medium at a concentration of 0.1 g/mL, and incubated at 37 °C for 24 h. The hydrogel extracts were sterilized via filtration (filter diameter = 220 nm). The sterilized extracts were mixed with equal volume of double-concentrated ECM culture medium containing 10% FBS to get 100% hydrogel extracts, and the 100% hydrogel extracts were mixed with ECM culture medium containing 5 vol % FBS to get 50% hydrogel extracts. HUVECs suspension (100 μL) was seeded on a 96-well culture plate at the number of 5000 cells per well. The 96-well plate was incubated at 37 °C in a 5% $CO_2$ humidified incubator for 24 h. Then, the medium was discarded and replaced with 100 μL of 100% extracts and 50% extracts. The ECM culture medium with 5 vol % FBS was used as a negative control and ECM culture medium with 5 vol% FBS and 0.7 wt% acrylamide was used as a positive control. The plate was incubated for 1 and 2 days. At the end of the culture time, 20 μL MTT solution (5.0 mg/mL) was added to the medium and continued to incubate for another 4 h, then the MTT medium was replaced by DMSO to dissolve the formazan crystals. Then the optical density (OD) of each well was read using a microplate reader at a wavelength of 490 nm. The cell viability of samples compared with the control was calculated from the following Eq.(1):

$$\text{Cell viability (\%)} = \frac{OD(\text{sample}) - OD(\text{positive})}{OD(\text{negative}) - OD(\text{positive})} \times 100 \quad (1)$$

### 2.8 Tissue compatibility evaluation

To evaluate the tissue compatibility of the SCTS scaffolds, SCTS hydrogel scaffolds (with a diameter of 8 mm and thickness of 3 mm) cross-linked with 1.5 units/mL HRP and 5 mM $H_2O_2$ were prepared. Then, the hydrogels were freeze-dried and immersed in 75% ethanol solution for 2 h to sterilization and then the scaffolds were rinsed several times with sterile saline. As a control, enzymatically cross-linked anionic CMCTS scaffolds were prepared as the same as the SCTS scaffolds prepared. And the cationic CTS scaffolds were used as another control and prepared in acetic acid solution. Briefly, CTS was dissolved in 1 vol% of acetic acid solution and then freeze-dried, then the freeze-dried scaffolds were immersed into 3 wt% NaOH solution, raised with PBS thoroughly, and then sterilized using 75% ethanol solution, and then raised with sterile saline thoroughly. After sterilization, all the scaffolds were implanted into the subcutaneous pockets of SD female mice (180–200 g) on symmetrical sides of the back. The incision was subsequently sutured to close (This part was entrusted to the Experimental Animal Center of Tianjin).

The implants were harvested at 4 intervals: 7, 14, 21 and 28 days after implanting. At each time point, each kind of scaffold with 3 parallel were taken out. Before the scaffolds were harvested, the mice were perfused with India ink in order to mark the blood vessels, after blood circulation for 5 minutes; the mice were narcotized and then killed. The implants were harvested and fixed in 10% of formaldehyde solution for 2 days, and then paraffin embedded, sectioned and stained with hematoxylin and eosin. The histologic sections were observed using an Olympus BX51 fluorescence microscope and photographed.

### 2.9 Statistical analysis

All data were expressed as means ± standard deviation (SD) for $n = 3$. Statistical analysis was performed using OriginPro 8.5. A two-tailed paired Student $t$ test was used to compare the difference. Significance was accepted at $p < 0.05$.

## 3 Results and discussion

Hydrogels can be formed by ionic cross-linking or by covalent cross-linking. When it comes to ionic cross-linking, the ions in the hydrogels could be exchanged with other ionic molecules in aqueous environment, resulting in an uncontrollable degradation of the hydrogel [11]. Compared with ionic cross-linking method, hydrogel formed by covalent cross-linking method would be more stable. However, the toxicity of cross-linking agent must be considered. The cross-linking agent should have no toxicity to the cells or tissues. Previously, a kind of glutaraldehyde cross-linked SCTS hydrogels (Glu-SCTS) were prepared [12]. However, the use of Glu-SCTS in biological application was limited to some extent due to the toxicity of cross-linking agent. Enzymatically cross-linked hydrogels had attracted much attention due to its unique advantage such as mild preparation conditions and low toxicity of the cross-linking agent. In this paper hydrogels of SCTS-HPA were prepared by oxidatively coupling the phenols on HPA in presence of HRP and $H_2O_2$.

### 3.1 Synthesis and characterization of SCTS and SCTS-HPA conjugate

The SCTS-HPA was prepared via two steps according to the literature as showed in Figure 1 [10]. First, SCTS was synthesis in $H_2SO_4/HSO_3Cl$ (1:2; *v*/*v*), and then SCTS-HPA was achieved by carbodiimide activation chemistry. The $M_w$ of SCTS was $4.7 \times 10^4$, determined by GPC. And the substitution degree (DS) of the $-SO_3-$ group was 89.47% determined by ICP ($-SO_3-$ groups per 100 glucosamine units). The conjugation of SCTS-HPA was confirmed by analysis of FTIR and $^1$H NMR. The new peak appeared at 1552 $cm^{-1}$ in the FTIR spectrum (Figure 2) of the SCTS-HPA was attributed by the typical stretching vibration of C–N of the amide band from SCTS-HPA. As compared with SCTS, new peaks at 6.9–7.2 ppm assigned to the aromatic protons of HPA appeared in the $^1$H NMR spectrum (Figure 3) of SCTS-HPA. These results indicated that the SCTS-HPA conjugate was successfully synthesized. The DS of HPA was calculated by $^1$H NMR and was shown to be approximately 5.5 HPA per 100 glucosamine units.

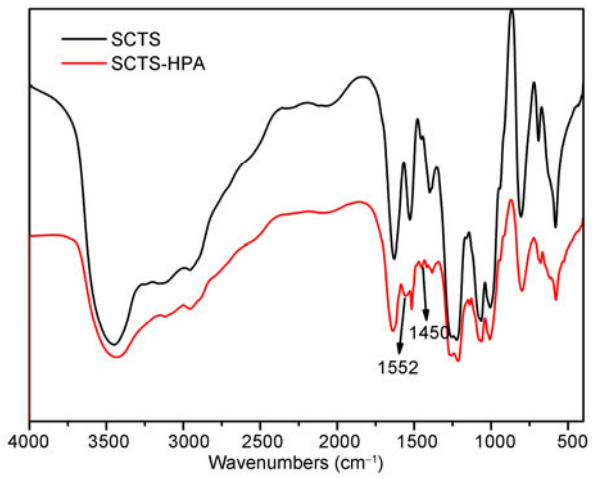


**Figure 2** FTIR spectrum of SCTS and SCTS-HPA.

### 3.2 Hydrogel preparation and gelation time test

Gelation time is very important for biomedical applications, such as drug delivery system, in situ forming hydrogels for tissue engineering. For example, faster gel rate was required for effectively encapsulation for protein, DNA, and drug, especially for injectable hydrogel target injection [13]. Previously it was reported that 1 min was an appropriate time for localized hydrogel formation and protein encapsulation [14]. Because slow gelation rate would cause undesired leakage of the protein to the surrounding tissues and compromise the therapeutic outcome. On the other hand, slower gelation time is required for the larger and irregular defect site hydrogel injection for tissue engineering use. And for slower hydrogel formation, it was reported that the phenolic hydroxyl containing material could form hydrogel even without HRP and $H_2O_2$ *in vivo* environment [15]. Here, the gelation time was determined using a vial tilting method [16]. Figure 4 showed the photographic images of the hydrogel formed before and after. Figure 5 showed the gelation time of SCTS hydrogels and that the gelation time depends on the concentration of HRP and $H_2O_2$, respectively. The gelation time decreased with the increasing of HRP concentration. On the contrary, the gelation time increased with the increasing of $H_2O_2$ concentration. In this study, the gelation time of hydrogel decreased from 196 to 22 s with

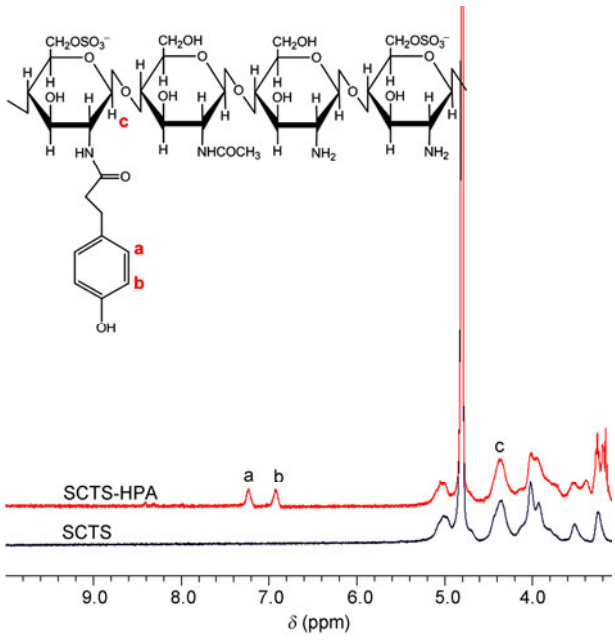


**Figure 3** $^1$H NMR spectrum of SCTS and SCTS-HPA.

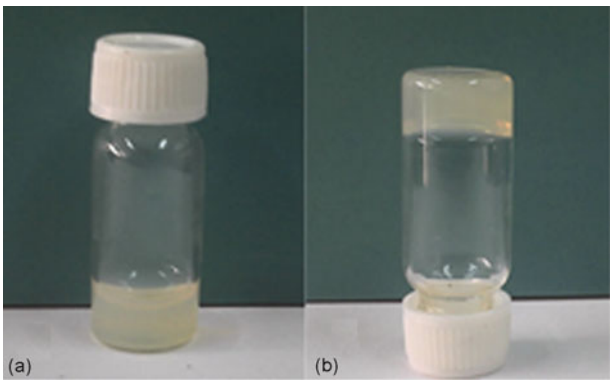


**Figure 4** The photographic images of the hydrogel formed before (a) and after (b).

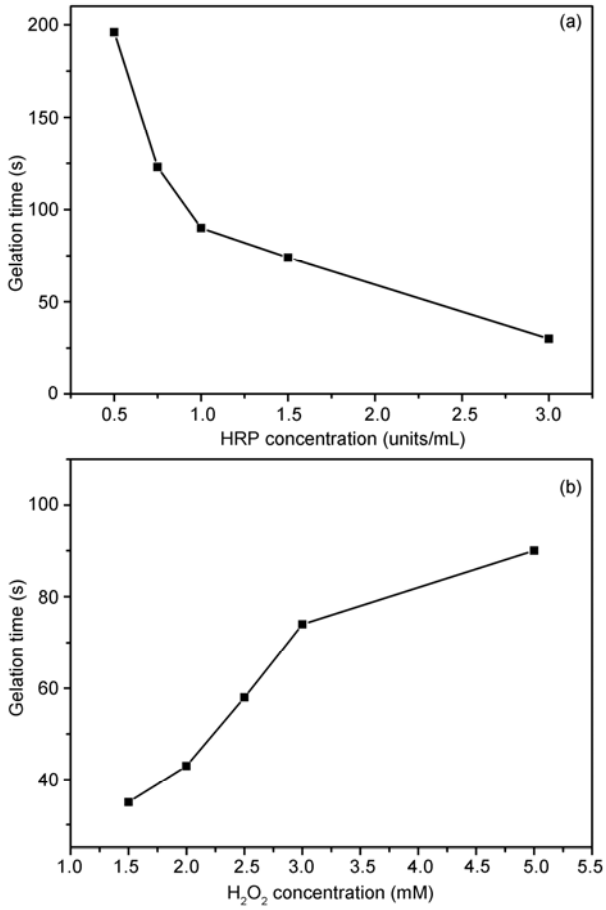


**Figure 5** Gelation time of SCTS-HPA hydrogels as a function of catalyst. (a) Effect of HRP with 3 mM $H_2O_2$ and 4 wt% SCTS; (b) effect of $H_2O_2$ with 1.5 units/mL HRP and 4 wt% SCTS.

the HRP concentration increasing from 0.5 to 3.0 units/mL at constant polymer (4 wt%) and $H_2O_2$ concentration (3.0 mM). In contrast, with the increasing of the concentration of $H_2O_2$ from 1.5 to 5.0 mM, the gelation time increased from 35 to 90 s at a constant concentration of polymer (4 wt%) and HRP (1.5 units/mL). The delay in gelation time of high concentration $H_2O_2$ was mainly due to the deactivation effect of $H_2O_2$ with high concentration on HRP and this effect would make HRP adopt an inactivated configuration [16]. This tendency of the gelation time was in agreement with many other studies [13, 16]. In short, the concentration of HRP and $H_2O_2$ can be easily changed for obtaining the desirable gelation time to satisfy the different requirement in biomedical application..

### 3.3 Rheological analysis

The mechanical properties of the hydrogels were measured by rheometer in 'time controlled oscillatory mode', and a series of elastic modulus ($G'$) ($G'$ indicates the stiffness of the materials) values of SCTS hydrogels were achieved by varying the $H_2O_2$ concentration at a constant HRP concentration (1.5 units/mL) and temperature (37 °C). Figure 6 exhibited that all the hydrogels' $G'$ reached a plateau within 150 s which indicated that the cross-linking was complete. And from Figure 6, it also showed that the $G'$ of the hydrogels increases with the $H_2O_2$ concentration increasing. For example, the $G'$ of hydrogel was 300 Pa with 1.5 mM $H_2O_2$ (the corresponding cross-linking density was approximately 32%, the cross-linking density was calculated by the concentration of $H_2O_2$ and HPA, $M_{H_2O_2}/2M_{HRP}$), the $G'$ increased to 1400 Pa with the $H_2O_2$ concentration was 2.5 mM (the corresponding cross-linking density was approximately 54%), and when the $H_2O_2$ concentration increased to 5.0 mM, the $G'$ was up to 5500 Pa (the corresponding cross-linking density was approximately 100%). These results could be explained by the restriction of the polymer chains' free motion with the increasing of cross-linking degree, so the hydrogel became more and more rigid. The mechanical property or stiffness of the scaffold was an important parameter for tissue engineering scaffold. And the mechanical strength of the scaffold should vary according to different use. For example, the mechanical strength should be high for bone scaffold, and the mechanical strength should be

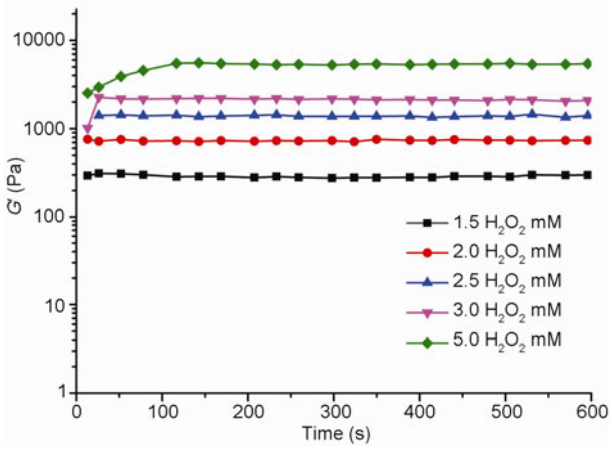


**Figure 6** The storage modulus ($G'$) of SCT-HPA hydrogels (4 wt% in PBS, pH 7.4) with different $H_2O_2$ concentration and constant HRP concentration (1.5 units/mL) at 37 °C.

low for soft tissue like liver. Kurisawa *et al.* [17] proved that the stiffness influenced the differentiation of mesenchymal stem cell. Here we prepared SCTS hydrogel scaffold which had elastic modulus ranged from hundreds Pa to thousands Pa could be used as several soft tissue engineering scaffolds, such as brain and liver which had elastic modulus in the few hundred Pa range and few thousands Pa range [18–21]. These results indicated that, the mechanical strength or stiffness of the hydrogels could be easily controlled by varying the $H_2O_2$ concentration.

### 3.4 Morphology of dehydrated SCTS-HPA hydrogels

A successful scaffold for tissue engineering was typically couple to appropriate transport of nutrients, proteins, cells, and waste products into and out of the scaffolds [22]. The pore size of the scaffold is one of the most important parameters for tissue engineering scaffold, because the pore size affects cells' biological functions. And many researchers had studied the effects of pore size on the cell behaviors. For example, Gibson *et al.* [23] prepared collagen glycosaminoglycan (CG) scaffolds with different pore size, and evaluated the relationship between cell attachment and viability and pore size. They found the scaffold with ~100 μm pore size was the optimum diameter for cellular adhesion and migration. In this work, the morphologies of the dehydrated SCTS-HPA hydrogels were imaged by SEM. Figure 7 showed the cross section of different samples. The samples exhibited interconnected, irregularly and macroporous sponge-like structures. The pore size decreased with the increasing concentration of $H_2O_2$. For example, the pore size of hydrogel was 183.78 μm with 1.5 mM $H_2O_2$ (Figure 7(a)), and the pore size dropped to 96.08 μm (Figure 7(c)) when the $H_2O_2$ concentration increased to 5 mM. This phenomena was also found in many other enzymatically cross-linked hydrogels by using HRP/$H_2O_2$ [13, 24]. The reason for this phenomenon was that more phenolic hydroxyl sections were oxidized with the increasing of oxidant ($H_2O_2$) concentration, thus the cross-linking density would increase and the distance between the molecular chains would be shorten, resulting in the decrease of the pore size of the hydrogel. In this study, scaffolds with different pore size could be obtained by changing the $H_2O_2$ concentration. And we used the scaffold with appropriate pore size (~100 μm) when the $H_2O_2$ was 5 mM in the subsequent experiment *in vivo*.

### 3.5 Cytotoxicity assay

The main reason for tissue inflammation and adverse reaction is the leachable substances existing in the polymer, generally including residual unreacted monomer, low molecular weight polymer, catalyst and other additives, etc [25]. Therefore, it is necessary to investigate the toxicity of the leachable substances in the polymer scaffold to the cells. In this study, HUVECs were chosen to evaluate the toxicity of the hydrogel extracts via MTT assay according to GB/T 16886.5-2003 (ISO10993-5:1999). Blood vessels existed in many organs and tissues to transport the nutrients, oxygen and metabolic substances, and endothelial cell were the indispensable part of the blood vessels. So the scaffold used as the substitutes of thick organs or tissues should have no cytotoxicity to the endothelial cells. Here we cultured HUVECs with hydrogel extracts and evaluated the influence of hydrogel extracts on HUVECs. Figure 8 showed the cell viability of the cells incubated with the 100% and 50% hydrogel extracts from the hydrogels with different crosslinking degree. The results showed that cell viability of different samples ranged from 85% to 110% after 24 h and 48 h incubation. According to the GB/T 16886.5-2003 (ISO10993-5:1999), samples with cell viability higher than 75% could be considered as no cytotoxicity. Although the cell viability of 48 h was lower than 24 h incubation, they did not show a significant difference on statistical level ($P > 0.5$). In order to eliminate the effects on cells viability from residual $H_2O_2$ in hydrogels, a control experiment was carried out. The hydrogels freshly prepared (cross-linked by 5 mM $H_2O_2$) were dialyzed against distilled water for 2 days, and then hydrogel extracts were prepared as the same as described above, and then the cytotoxicity on HUVECs was evaluated. The results showed that the cell viability had no significant dif-

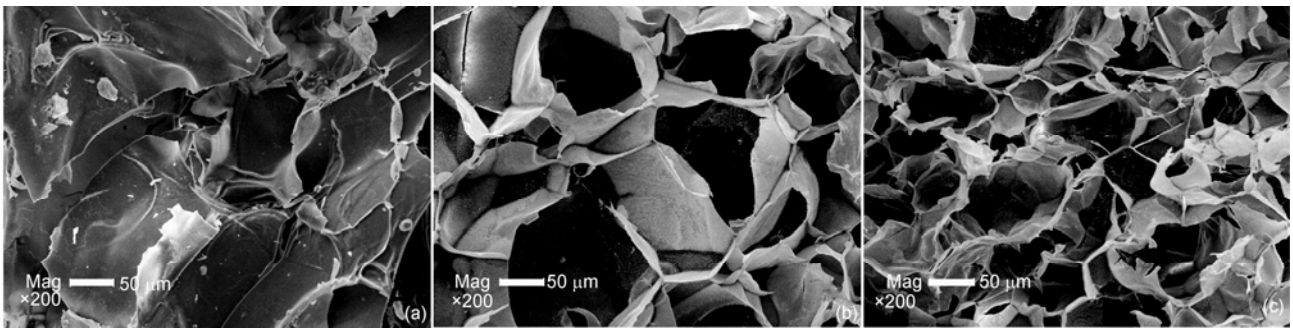


**Figure 7** The cross section SEM images of lyophilized scaffold with polymer concentration 4 wt% and HRP concentration 1.5 units/mL and different $H_2O_2$ concentration. (a) 1.5 mM $H_2O_2$, (b) 2.5 mM $H_2O_2$, (c) 5.0 mM $H_2O_2$, scale bar = 50 μm.

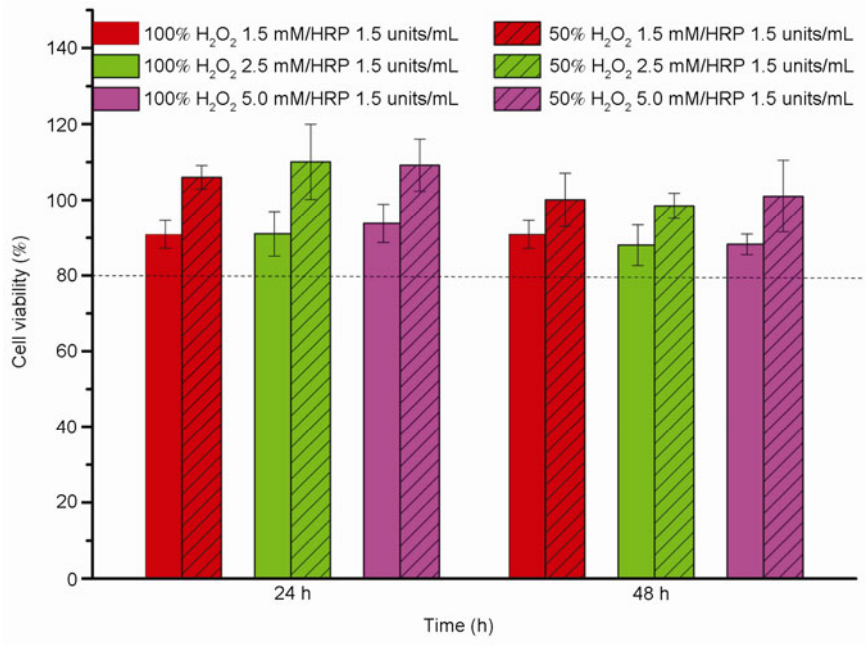


**Figure 8** Viability of HUVEC cultured with hydrogel extracts on 24 h and 48 h.

ference to the hydrogel extracts without dialysis treatment (data not shown). The result indicated that most of $H_2O_2$ had been reacted in hydrogel, and the concentration of residual $H_2O_2$ was very low. In fact, it had been reported that $H_2O_2$ did not show cytotoxicity when its concentration below 5 μM [26]. Therefore, the residual $H_2O_2$-induced cytotoxicity could be ignored in this study. In conclusion, the enzymatically crosslinked SCTS scaffold showed no cytotoxic to HUVECs in our condition, and it was expected to be used as blood vessel containing tissue engineering scaffold.

### 3.6 Tissue compatibility evaluation

Vascularization is the key challenge in thick tissue engineering [27]. Many approaches had been tried to solve this problem. Biologically derived and synthetic materials had been prepared into vascular scaffold to induce or support blood vessels formation, such as decellularized matrix, natural and synthetic polymers [28–30]. One of the major obstacles to fabricate a successful vascular scaffold was the scaffolds' thrombus formation via platelet deposition. So the materials used for vascular scaffold must possess anticoagulant quality. Many researchers had used CTS or modified CTS to fabricate scaffold used for thick tissues enginnering, such as liver [31]. However, CTS was a kind of positive charged material, thus it had the risk to promote thrombus formation [3]. CMCTS was a derivative of CTS and had been reported to have no influence on the blood system of rats, including coagulation function, anticoagulation performance [32]. Here, we prepared SCTS and other two kinds of scaffolds as control which were positive charged CTS scaffold and negative charged CMCTS. SCTS scaffold used here was crosslinked by 1.5 units/mL HRP and 5.0 mM $H_2O_2$ which had the maximum mechanical strength (5500 pa) and the optimum pore size for cell adhesion and migration (~100 μm). CMCTS scaffold was prepared as the same as the SCTS scaffold. CTS scaffold was prepared in acetum as described above. Then, all kinds of scaffolds were sterilized and implanted into the subcutaneous pockets of SD mice to evaluate the tissue compatibility of the scaffold for thick tissue engineering scaffold use. During the experiment period, three mice in CTS group and two in CMCTS group appeared skin necrosis. Meanwhile, no adverse phenomenon was observed in SCTS group for 28 days. Figure 9 showed the representative pictures of the necrotic skin in the CTS and CMCTS group, compared with the intact skin of SCTS group. The reason of the skin necrosis maybe the thrombus formation in CTS and CMCTS scaffolds. The inference was confirmed by H&E-stained histologic sections showed in Figure 10. Figure 10 showed the representative H&E-stained histologic sections of the different scaffolds. From the sections we saw the CTS group formed serious thrombus after the scaffold implantation for 4 weeks (Figure 10(a)), and the thrombus was filled with the whole scaffold. The CMCTS group showed some tissue penetration, however also appeared thrombus to some extent after scaffold implantation (Figure 10(b)). Although the thrombus formed in CMCTS group was less serious, CMCTS scaffold resulted in thrombus formation indeed and the mice appeared skin necrosis due to the scaffold implantation. In SCTS group (Figure 10(c)), the tissue penetrated into the scaffold on the day 28, and there were many blood vessels within the tissue. According to our results, the negative charged CMCTS appeared serious thrombus, though

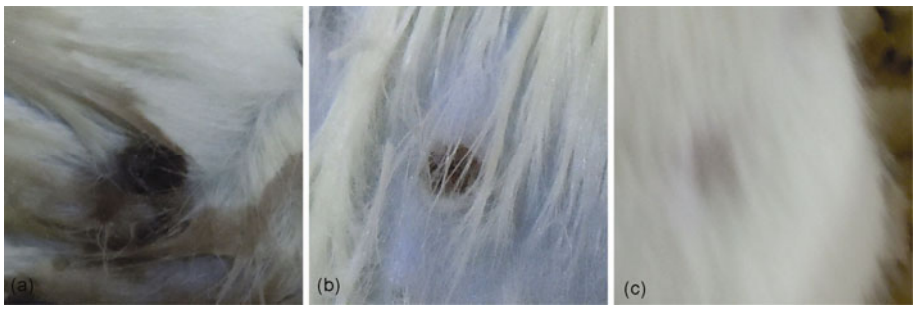


**Figure 9** Representative pictures of the necrotic skin after the scaffolds implanted for 4 weeks from CTS group (a), CMCTS group (b), and SCTS group (c).

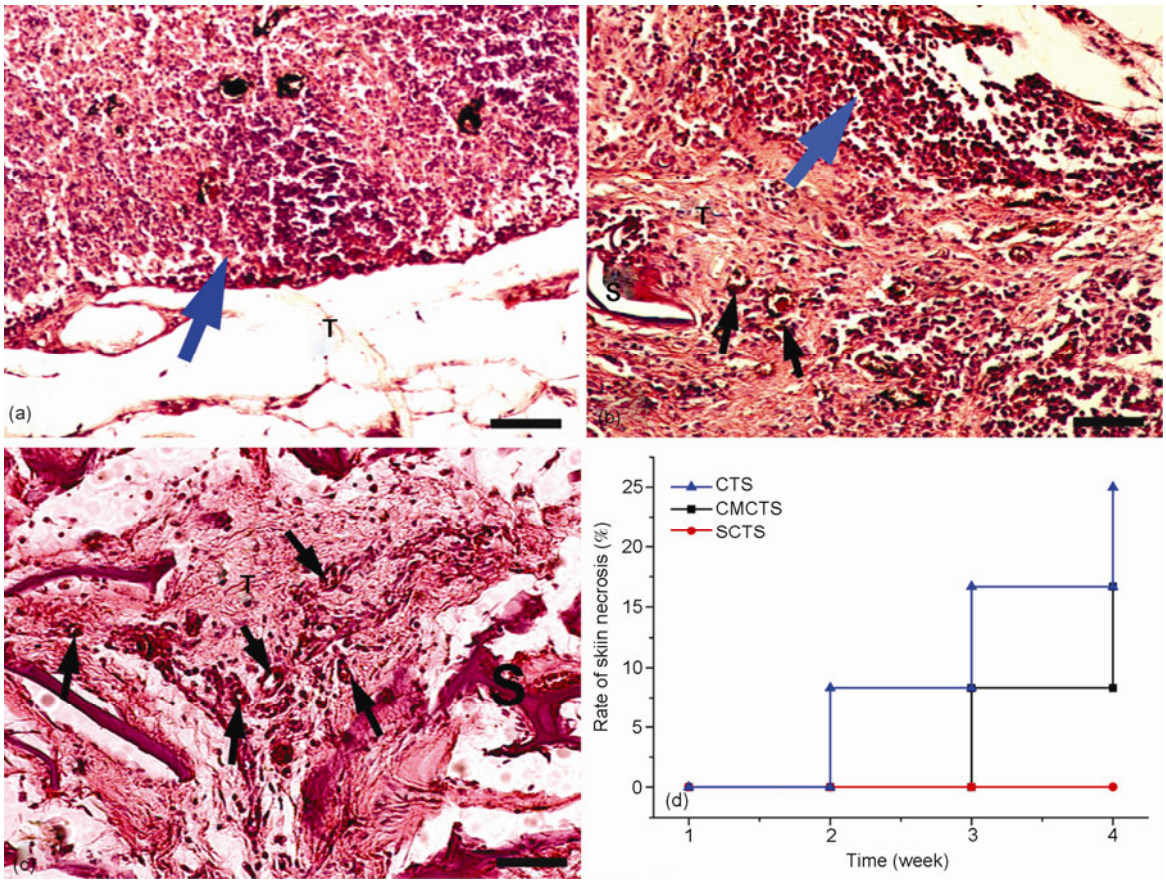


**Figure 10** Representative H&E-stained histologic sections of CTS (a), CMCTS (b), SCTS (c) scaffold implanted in mice for 4 weeks. And the rate of skin necrosis after the scaffold implantation (d). Blue coarse arrows denote thrombi in the scaffolds, black fine arrows denote blood vessels in the scaffold, S indicates scaffold and T indicates tissue. Scale bar = 100 μm.

the possibility and appear time of thrombus was lower and later than CTS group (16.7% vs. 25%, 21d vs. 14d in Figure 10(d)). These finding indicated that the negative charged CMCTS was not suitable for using as blood vessel containing thick tissue engineering scaffold, and this conclusion was opposite to previous report [32]. On the other hand, the negative charged SCTS which proved to have anticoagulant property previously showed no signs of thrombus formation and also induced and supported tissue penetration and blood vessels growth in our work. These results indicated that the SCTS scaffold can be safely used as vascular scaffold and thick tissue engineering scaffold.

## 4 Conclusions

A kind of enzymatically cross-linked SCTS hydrogel scaffold was successfully prepared in this work. The formation time, pore size, and mechanical strength of the hydrogel could be easily regulated by changing the concentration of HRP/$H_2O_2$. The cytotoxicity results of the hydrogel extracts showed that the hydrogel had no cytotoxicity to HUVECs.

*In vivo* studies showed that SCTS scaffold could induce tissue penetration and support new blood vessels growth. Furthermore, SCTS hydrogel did not cause thrombus formation. These results indicated that the SCTS hydrogel scaffold has great potential for thick tissue engineering.

*This work was financially supported by the National Basic Research Program of China (973 Project, 2011CB606202) and the National Natural Science Foundation of China (51273095).*

1 Jain RK, Au P, Tam J，Duda DG, Fukumura D. Engineering vascularized tissue. *Nat Biotechnol*, 2005, 23: 821–823
2 Singh DK, Ray AR. Biomedical applications of chitin, chitosan, and their derivatives. *J Macromol Sci. Part* C: *Polymer Reviews,* 2000, 40: 69–83
3 Amiji MM. Surface modification of chitosan membranes by complexation-interpenetration of anionic polysaccharides for improved blood compatibility in hemodialysis. *J Biomater Sci Polym Ed*, 1996, 8: 281–98
4 Chen XG, Park HJ. Chemical characteristics of *O*-carboxymethyl chitosans related to the preparation conditions. *Carbohyd Polym*, 2003, 53: 355–359
5 Davis SS, Lin W, Bignotti Fabio, Ferruti P. Conjugate of polyethylene glycol and chitosan. United State Patent, US 6730735 B2, 2004-05-04
6 Jayakumar R, New N, Tokura S, Tamura H. Sulfated chitin and chitosan as novel biomaterials. *Int J Biol Macromol*, 2007, 40: 175–181
7 Mariappan MR, Alas EA, Williams JG, Prager MD. Chitosan and chitosan sulfated have opposing effects on collagen-fibroblast interactions. *Wound Repair Regen*, 1999, 7: 400–406
8 Li QL, Huang N, Chen JL, Chen C, Chen JY. Endothelial cell and platelet behavior on titanium modified with a mutilayer of polyelectrolytes. *J Bioact Compat Pol*, 2009, 24: 129–150
9 Terbojevich M, Carraro C, Cosani A. Solution studies of chitosan 6-O-sulfate. *Makromol Chem*, 1989, 190: 2847–2855
10 Tian Q, Wang XH, Wang W, Zhang CN, Wang P, Yuan Z. Self-assembly and liver targeting of sulfated chitosan nanoparticles functionalized with glycyrrhetinic acid. *Nanomedicine*, 2012, 8: 870–879
11 LeRoux MA, Guilak F, Setton LA. Compressive and shear properties of alginate gel: Effects of sodium ions and alginate concentration. *J Biomed Mater Res*, 1999, 47: 46–53
12 Lin RZ, Miao J, Dong SX. Synthesis and Properties of pH-sensitive Sulfated Chitosan(SCS) Hydrogels. *J Mater Sci Eng*, 2008, 26: 950–953
13 Park KM, Shin YM, Joung YK, Shin H, Park KD. *In situ* forming hydrogels based on tyramine conjugated 4-Arm-PPO-PEO via enzymatic oxidative reaction. *Biomacromolecules*, 2010, 11: 706–712
14 Lee F, Chung JE, Kurisawa M. An injectable hyaluronic acid-tyramine hydrogel system for protein delivery. *J Control Release*, 2009, 134: 186–193
15 Kurisawa M, Chung JE, Yang YY, Gao SJ, Uyama H. Injectable biodegradable hydrogels composed of hyaluronic acid-tyramine conjugates for drug delivery and tissue engineering. *Chem Commun*, 2005, 14: 4312–4314
16 Sakai S, Kawakami K. Synthesis and characterization of both ionically and enzymatically cross-linkable alginate. *Acta Biomater*, 2007, 3: 495–501
17 Wang LS, Boulaire J, Chan PP, Chung JE, Kurisawa M. The role of stiffness of gelatin–hydroxyphenylpropionic acid hydrogels formed by enzyme-mediated crosslinking on the differentiation of human mesenchymal stem cell. *Biomaterials*, 2010, 31: 8608–8616
18 Hirakawa K, Hashizume K, Hayashi T. Viscoelastic property of human brain-for the analysis of impact injury. *No To Shinkei*, 1981, 33: 1057–1065
19 Miller K, Chinzei K, Orssengo G, Bednarz P. Mechanical properties of brain tissue *in-vivo*: Experiment and computer simulation. *J Biomech*, 2000, 33: 1369–1376
20 Evans DW, Moran EC, Baptista PM, Soker S, Sparks JL. Scale-dependent mechanical properties of native and decellularized liver tissue. *Biomech Model Mechanobiol*, 2012, DOI 10.1007/s10237-012-0426-3
21 Chen F, Tian M, Zhang DM, Wang JY, Wang QG, Yu XX, Zhang XH, Wan CX. Preparation and characterization of oxidized alginate covalently cross-linked galactosylated chitosan scaffold for liver tissue engineering. *Mat Sci Eng C-Bio S*, 2011, 32: 310–320
22 Drury JL, Mooney DJ. Hydrogels for tissue engineering: scaffold design variables and applications. *Biomaterials*, 2003, 24: 4337–4351
23 O'Brien FJ, Harley BA, Yannas IV, Gibson LJ. The effect of pore size on cell adhesion in collagen-GAG scaffolds. *Biomaterials*, 2005, 26: 433–441
24 Lee F, Chung JE, Kurisawa M. An injectable enzymatically crosslinked hyaluronic acid–tyramine hydrogel system with independent tuning of mechanical strength and gelation rate. *Soft Matter*, 2008, 4: 880–887
25 Rosiak J, Olejniczak J, Pekala W. Fast reaction of irradiated polymers—I. Crosslinking and degradation of polyvinylpyrrolidone. *Int J Radiat Appl Instrum C Radiat Phys Chem*, 1990, 36: 747–755
26 Jonas SK, Riley PA, Willson RL. Hydrogel peroxide cytotoxicity. Low-temperature enhancement by ascorbate or reduced lipoate. *Biochem J*, 1989, 264: 651–655
27 Novosel EC, Kleinhans C, Kluger PJ. Vascularization is the key challenge in tissue engineering. *Adv Drug Deliv Rev*, 2011, 63: 300–311
28 Ott HC, Matthiesen TS, Goh SK, Black LD, Kren SM, Netoff TI, Taylor DA. Perfusion-decellularized matrix: Using nature's platform to engineer a bioartificial heart. *Nat Med*, 2008, 14: 213–221
29 Yu J, Gu Y, Du KT, Miharda S, Sievers RE, Lee RJ. The effect of injected RGD modified alginate on angiogenesis and left ventricular function in a chronic rat infarct model. *Biomaterials*, 2009, 30: 751–756
30 Cai K, Kong T, Wang L, Liu P, Yang W, Chen C. Regulation of endothelial cells migration on poly (D, L-lactic acid) films immobilized with collagen gradients. *Colloids Surf B Biointerfaces*, 2010, 79: 291–297
31 Li J, Pan J, Zhang L, Yu Y. Culture of hepatocytes on fructose-modified chitosan scaffolds. *Biomaterials*, 2003, 24: 2317–2322
32 Fu D, Han B, Dong W, Yang Z, Lv Y, Liu W. Effects of carboxymethyl chitosan on the blood system of rats. *Biochem Biophys Res Commun*, 2011, 408: 110–114